Empirical determination of intermediate-coupling amplitudes and transition rates from spectroscopic data

L. J. Curtis, Z. B. Rudzikas,* and D. G. Ellis
Department of Physics and Astronomy, University of Toledo, Toledo, Ohio 43606
(Received 7 December 1990; revised manuscript received 1 February 1991)

A simple general method is presented whereby measured spectroscopic energy-level data can be used to empirically construct the eigenvectors of intermediate coupling for an arbitrary configuration. These empirical eigenvectors can be used to elucidate the transition rates into, out of, and among the levels of the configuration by separating the effects of intermediate coupling from the radial transition moment. Predictive applications to the np^3 configurations of the N and P isoelectronic sequences are presented.

Spectroscopic energy levels can be measured to very high precision, and observations for a relatively small number of isoelectronic ions can often be reliably interpolated and extrapolated [1] to provide a comprehensive database for the entire isoelectronic sequence. Transition probabilities and oscillator strengths can seldom be measured to better than 1%, and a comprehensive database for these quantities is more difficult to generate. It has been shown earlier [2] that intermediate-coupling amplitudes can be deduced from observed spectroscopic energy-level data and used to accurately specify transition probabilities either in a wholly empirical manner, or in combination with single-particle semiempirical computations. The methods presented in Ref. [2] were restricted to systems in which only two LS coupling terms were mixed by intermediate coupling. The purpose of this Brief Report is to show that these methods can be extended to systems of arbitrary complexity. Applications of the method to the np^3 ground configurations of the N and P isoelectronic sequences are presented.

In the single-configuration picture of an atomic system, intermediate-coupling effects are manifested in both the energy-level values and the transition rates. By a simple general procedure described below, the measured values for energy-level spacings within a configuration can be used to construct the eigenvectors of its intermediate coupling. These eigenvectors can then be used to elucidate line strengths, oscillator strengths, and transition probabilities in either of two ways: they can be used in conjunction with single-electron LS-coupling equations to make empirical computations, or they can be used to remove the effects of intermediate coupling from predictive semiempirical expositions of measured values.

For a given configuration, energy levels can be specified [3,4] as a function of the electron-electron direct and exchange Slater energies F^k and G^k, the spin-orbit energy ζ, and the electron-nucleus central energy E^0. Expressed in terms of LS basis states, intermediate coupling mixes states of the same total angular momentum J. If there are N states with the same value of J in a given configuration, their energies are specified by an $N\times N$ symmetric nondiagonal submatrix M_{ij} which can be diagonalized by a transformation T_{ij}, where

$$\sum_{n=1}^{N}\sum_{m=1}^{N} T_{in}M_{nm}T_{mj}^{-1}=E_i\delta_{ij} \ . \tag{1}$$

The eigenvalues E_i are given by the N roots of λ in the equation

$$\det(M_{ij}-\lambda\delta_{ij})=0 \ , \tag{2}$$

which yields the secular equation

$$\sum_{n=0}^{N} a_n\lambda^n=0 \ , \tag{3}$$

where $a_N=1$. Although the explicit solution for E_i in terms of the a_n for $N>2$ can be very complicated and cumbersome, the inverse solution is quite simple. The a_n coefficients can be written directly as sums and products of the experimentally determined real eigenvalues E_i given by [5]

$$\begin{aligned} a_{N-1}&=-\sum_{i=1}^{N}E_i \ , \\ a_{N-2}&=\sum_{i=1}^{N}\sum_{j>i}^{N}E_iE_j \ , \\ a_{N-3}&=-\sum_{i=1}^{N}\sum_{j>i}^{N}\sum_{k>j}^{N}E_iE_jE_k \ , \\ &\vdots \\ a_0&=(-1)^N\prod_{i=1}^{N}E_i \ . \end{aligned} \tag{4}$$

These equations permit the a_n coefficients to be determined from the experimental energies. Although there are N^2 matrix elements M_{ij} and only N coefficients a_n, the matrix elements are interrelated by the p Slater parameters, and it is possible to construct the M_{ij} from the a_n for a specific J value if $p\le N$. Additional relationships among the Slater parameters can be obtained from other values of J within the configuration. If p is less than the total number of levels in the configuration, the Slater pa-

rameters are overdetermined, which provides tests of the single-configuration assumption. Once M_{ij} has been determined from the experimental data, the transformation T_{ij} can be computed using

$$\sum_{n=1}^{N} T_{in}M_{nj}=E_iT_{ij} , \tag{5}$$

and the eigenvectors are then given by

$$|\psi_i\rangle=\sum_{j=1}^{N} T_{ij}|j\rangle , \tag{6}$$

where $|j\rangle$ denotes the LS basis states and $|\psi_i\rangle$ denotes the intermediate coupled physical states. The applications presented in Refs. [2] involved 2×2 matrices, but the general formulation presented above can easily be applied to 3×3, 4×4, or even larger arrays, provided that the number of Slater parameters involved does not exceed the number of levels in the configuration.

In terms of the matrix elements, the transition probabilities for electric ($E1$) and magnetic ($M1$) dipole transitions are given by [3]

$$(2J_k+1)A_{E1}(k,i)=(2.0261\times10^{-6}\ \mathrm{cm}^3/\mathrm{s})\times[E(k)-E(i)]^3S_{E1}(i,k) , \tag{7}$$

where

$$S_{E1}(i,k)=\left|\sum_{n=1}^{N}\sum_{m=1}^{N} T_{in}T_{km}\langle n\|\mathbf{r}\|m\rangle\right|^2 \tag{8}$$

and

$$(2J_k+1)A_{M1}(k,i)=(2.6973\times10^{-11}\ \mathrm{cm}^3/\mathrm{s})\times[E(k)-E(i)]^3S_{M1}(i,k) , \tag{9}$$

where

$$S_{M1}(i,k)=\left|\sum_{n=1}^{N}\sum_{m=1}^{N} T_{in}T_{km}\langle n\|\mathbf{J}+\mathbf{S}\|m\rangle\right|^2 . \tag{10}$$

Here $\mathbf{r}$ is in units of the Bohr radius and $\mathbf{J}$ and $\mathbf{S}$ are in units of Planck's constant $\hbar$. For $E1$ transitions, radial wave functions can be obtained from a variety of semiempirical methods [6] that derive wave functions from empirical data (e.g., the quantum-defect method, the Hartree-Slater potential, etc.). For pure LS coupling, $M1$ transition elements connect only states that differ at most in the J quantum number and depend only on angular and not radial quantities. They are given by the simple formulas [7]

$$\langle LSJ\|\mathbf{J}+\mathbf{S}\|LSJ\pm1\rangle=\{[(L+S+1)^2-J_>^2]\times[J_>^2-(L-S)^2]/4J_>\}^{1/2} ,$$
$$\langle LSJ\|\mathbf{J}+\mathbf{S}\|LSJ\rangle=[S(S+1)-L(L+1)+3J(J+1)]\times[(2J+1)/4J(J+1)]^{1/2} . \tag{11}$$

The p^3 configuration provides a particularly challenging case for the semiempirical specification of Slater parameters, since the energy levels for this half-filled subshell have no linear dependence on the spin-orbit parameter ζ that leads to its intermediate coupling. For this case, the energy matrix $\mathcal{H}$ is given (relative to the $^2P_{1/2}$ level) by [3,4]

$$\mathcal{H}=E^0+\frac{6}{25}F^2+\begin{array}{c} \\ {}^2D_{5/2} \\ {}^4S_{3/2} \\ {}^2D_{3/2} \\ {}^2P_{3/2} \\ {}^2P_{1/2} \end{array}\begin{array}{c}\begin{array}{ccccc} {}^2D_{5/2} & {}^4S_{3/2} & {}^2D_{3/2} & {}^2P_{3/2} & {}^2P_{1/2} \end{array}\\ \begin{pmatrix} -\frac{6}{25}F^2 & 0 & 0 & 0 & 0 \\ 0 & -\frac{3}{5}F^2 & 0 & \zeta & 0 \\ 0 & 0 & -\frac{6}{25}F^2 & \frac{\sqrt{5}}{2}\zeta & 0 \\ 0 & \zeta & \frac{\sqrt{5}}{2}\zeta & 0 & 0 \\ 0 & 0 & 0 & 0 & 0 \end{pmatrix}\end{array} . \tag{12}$$

We shall henceforth designate the $^2D_{5/2}$, $^4S_{3/2}$, $^2D_{3/2}$, $^2P_{3/2}$, and $^2P_{1/2}$ levels in indices by the labels $D5$, S, D, P, and $P1$. The E^0 dependence (which includes both the electron-nucleus and F^0 interactions) will be removed from the analysis that follows by defining the eigenenergies E_i relative to the unmixed $^2P_{1/2}$ energy. Applying Eq. (2) to diagonalize the $J=3/2$ submatrix yields the secular equation

$$0=\lambda^3+(\tfrac{21}{25}F^2)\lambda^2+[\tfrac{18}{125}(F^2)^2-\tfrac{9}{4}\zeta^2]\lambda-(\tfrac{99}{100}F^2\zeta^2) . \tag{13}$$

Using Eqs. (4), (5), and (6), it follows that

$$a_2=\tfrac{21}{25}F^2=-E_S-E_D-E_P ,$$
$$a_1=\tfrac{18}{125}(F^2)^2-\tfrac{9}{4}\zeta^2=E_SE_D+E_DE_P+E_PE_S , \tag{14}$$
$$a_0=-\tfrac{99}{100}F^2\zeta^2=-E_SE_DE_P ,$$

with the additional condition from the $J=5/2$ level [since the coefficient of λ^3 in Eq. (13) is unity, this can be denoted by a_3],

$$a_3=-\tfrac{6}{25}F^2=E_{D5} . \tag{15}$$

Since there are four equations and only two Slater parameters, the system is overdetermined. The data can be re-

duced by least-squares adjustment of the quantities F^2 and ζ so as to minimize the quantity

$$\chi^2=\sum_{i=0}^{3}[a_i(E)-a_i(F^2,\zeta)]^2W_i\ , \tag{16}$$

where $a_i(E)$ denotes the measured forms and $a_i(F^2,\zeta)$ denotes the parametrized forms of Eqs. (14) and (15), and W_i is a weighting factor that accounts for the relative sizes of the propagated experimental uncertainties. If the $a_i(E)$ values are all assumed to have the same relative uncertainties, the weights are given by

$$W_i=[a_i(E)]^{-2}\ . \tag{17}$$

The eigenvector amplitudes T_{ij} will be denoted here by $\langle\psi_i|j\rangle$ to emphasize their role in generating the ith eigenvector from the j basis states. Using the $J=3/2$ submatrix of Eqs. (12) and (5) yields

$$(\langle\psi_i|S\rangle,\langle\psi_i|D\rangle,\langle\psi_i|P\rangle)=(b_S,b_D,1)/(1+b_S^2+b_D^2)^{1/2}\ , \tag{18}$$

where

$$b_S(E_i)\equiv\zeta/(\tfrac{3}{5}F^2+E_i),\quad b_D(E_i)\equiv\frac{\sqrt{5}}{2}\zeta/(\tfrac{6}{25}F^2+E_i)\ . \tag{19}$$

(There are various phase ambiguities due, e.g., to the sign of the root of ζ^2, but these do not affect the magnitudes of the various inner products.) These eigenvectors can be combined with Eqs. (9)–(11) to predict $M1$ transition rates among these intermediate coupled levels.

We have applied this method to the $2s^22p^3$ ground-state configuration of the N isoelectronic sequence using both experimental and *ab initio* theoretical data. To illustrate the use of the method, consider the Fe^{19+} ion. Relative to the $^2P_{1/2}$ level, the measured energy-level data [8] for this ion are (in cm^{-1}) $E_S=-260\,090$, $E_D=-121\,820$, $E_{D5}=-84\,280$, and $E_P=63\,090$. For these measured values, the coefficients in the secular equation are given by Eqs. (14) to be $a_2=318\,820$, $a_1=7.5895\times10^9$, and $a_0=-1.9990\times10^{15}$, and Eq. (15) yields $a_3=-84\,280$. Weighted least-squares adjustment of the effective Slater parameters to these four a_i values using Eqs. (16) and (17) yields $F^2=370\,157$ cm^{-1} and $\zeta=73\,568$ cm^{-1}, which correspond to reconstructed energy-level separations given by $E_S=-248\,371$, $E_D=-125\,957$, $E_{D5}=-88\,838$, and $E_P=63\,397$. With these values for F^2 and ζ, the eigenvectors obtained from Eqs. (18) and (19) are

$$\begin{aligned}|S'\rangle&=-0.9279|S\rangle-0.1709|D\rangle+0.3314|P\rangle\ ,\\ |D'\rangle&=0.3003|S\rangle-0.8694|D\rangle+0.3924|P\rangle\ ,\\ |P'\rangle&=0.2211|S\rangle+0.4636|D\rangle+0.8580|P\rangle\ .\end{aligned} \tag{20}$$

These eigenvectors were combined with Eqs. (9)–(11) to obtain the $M1$ transition probabilities connecting the levels within this configuration. The results are presented in Table I, where they are compared with *ab initio* values computed both by us using the Cowan program [3], and by Cheng, Kim, and Desclaux [9].

The quantitative agreement among the three methods as shown in Table I is clearly quite good. The *ab initio* calculations include configuration interaction, but do not reproduce the experimental wavelengths. The empirical calculations are explicitly based on the single-configuration picture, but include configuration interaction implicitly through the use of experimental wavelengths. Configuration-interaction effects could also be included explicitly by introducing additional parameters into the matrix of Eq. (12) (e.g., the $2p^5\,^2P$ levels could be included by adding one more row, one more column, and one more parameter to the $J=3/2$ submatrix). However, Table I indicates that our two-parameter empirical fits reproduce *ab initio* theoretical calculations to within discrepancies in the latter, and the introduction of additional parameters is not justified on the basis of existing information.

A similar application was made to the levels of the $3s^23p^3$ ground configuration in the P isoelectronic sequence. For this sequence, comprehensive calculations of

TABLE I. $M1$ transition probabilities connecting the $2s^22p^3$ levels in Fe^{19+} (s^{-1}). HFR-CI denotes Hartree-Fock-relativistic with configuration interaction.

	Empirical[a]	Observed[b]	HFR-CI[c]		MCDF[d]	
Transition	$A(s^{-1})$	λ (Å)	A (s^{-1})	λ (Å)	A (s^{-1})	λ (Å)
$^4S_{3/2}$-$^2D_{3/2}$	1.88×10^4	723	1.62×10^4	710	1.75×10^4	707
$^4S_{3/2}$-$^2D_{5/2}$	1.71×10^3	569	1.36×10^3	548	1.33×10^3	561
$^4S_{3/2}$-$^2P_{1/2}$	3.48×10^4	384	3.15×10^4	385	3.26×10^4	385
$^4S_{3/2}$-$^2P_{3/2}$	3.05×10^4	309	2.99×10^4	308	2.91×10^4	309
$^2D_{3/2}$-$^2D_{5/2}$	4.31×10^2	2664	5.80×10^2	2393	3.95×10^2	2714
$^2D_{3/2}$-$^2P_{1/2}$	5.00×10^3	821	5.66×10^3	842	5.52×10^3	846
$^2D_{3/2}$-$^2P_{3/2}$	4.30×10^4	541	4.39×10^4	544	4.29×10^4	550
$^2D_{5/2}$-$^2P_{3/2}$	1.11×10^4	679	1.13×10^4	705	1.22×10^4	689
$^2P_{1/2}$-$^2P_{3/2}$	1.66×10^3	1585	1.76×10^3	1541	1.64×10^3	1570

[a]This work.
[b]Corliss and Sugar, Ref. [8].
[c]This work, using the program of Cowan, Ref. [3].
[d]Cheng, Kim, and Desclaux, Ref. [9].

both the energy levels and the line strengths for all charged ions have been made by Huang [10]. We have used this theoretical energy-level data base to deduce from Eqs. (14)–(19) the eigenvectors for the $J=3/2$ levels, and computed from them the empirical $M1$ line strengths for intermediate coupling using Eqs. (10) and (11). These empirical line strengths are compared with the corresponding multiconfiguration Dirac-Fock (MCDF) [10] computations for $25 \leq Z \leq 70$ in Fig. 1. (For $Z<25$ the mixing is small; for $Z>70$, avoided crossings with other configurations occur, and the labeling scheme [11] of Ref. [10] tabulates some inappropriate eigenvectors thereafter.)

The excellent agreement between the empirical and MCDF results exhibited by all of the nine possible intraconfiguration line strengths in Fig. 1 indicates that the dynamical behavior of these transitions is primarily governed by the singlet-triplet mixing, and that the degree of this mixing can be deduced from energy-level data in the single-configuration picture. At high Z, intermediate coupling is more important than configuration interaction, and the angular momentum vectors approach pure jj coupling (for $Z=70$ the empirical mixing amplitudes were within an additive increment of ± 0.04 from the jj-coupling values). For $M1$ transitions, the radial wave functions enter only through the monopole overlap integral and higher-order relativistic corrections to the magnetic dipole operator. While these corrections to the radial wave functions increase sharply with Z, Fig. 1 indicates that they have a negligible effect on the $M1$ line strengths. At lower Z, strong configuration-interaction effects (with, e.g., the $3p^5$ configuration) are expected, but Fig. 1 suggests that these enter as a secondary influence, by altering energy separations of the singlet and triplet levels of the same J, while retaining the singlet-triplet mixing amplitudes within the $3s^2 3p^3$ configuration as the primary factor in the characterization of the $M1$ transition rates.

The results presented here indicate that it is possible to deduce the eigenvector composition of a configuration in intermediate coupling easily and directly from spectroscopic energy-level data. Although the formalism is based on a single-configuration picture, the use of physical energy-level data accounts to some degree for effects of configuration interaction. The method provides a means both for extending semiempirical calculations of transition rates to more complex systems and of removing the effects of intermediate coupling from predictive expositions of measured data.

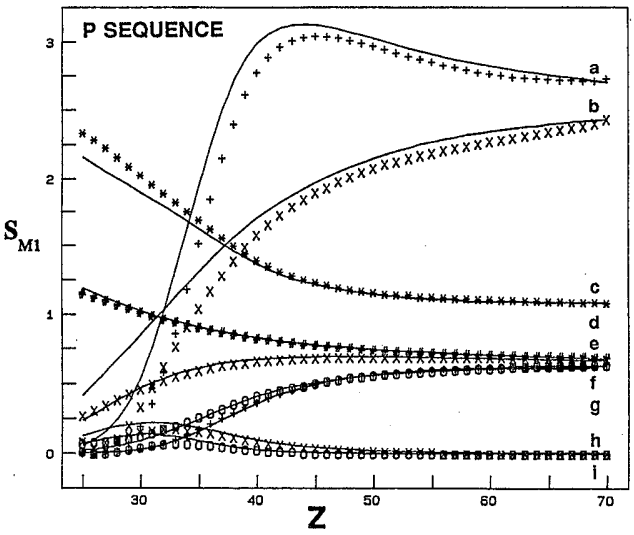

FIG. 1. Isoelectronic plot of the $M1$ line strengths S_{M1} among the levels of the $3s^2 3p^3$ ground configuration of the P sequence. The solid lines indicate *ab initio* calculations (Ref. [10]) whereas the symbols denote the empirical predictions made using Eqs. (10)–(19) and the energy-level values of Ref. [10]. Transitions are labeled as follows: (a) $^4S_{3/2}$-$^2D_{3/2}$, (b) $^2D_{3/2}$-$^2P_{3/2}$, (c) $^2D_{3/2}$-$^2D_{5/2}$, (d) $^2P_{1/2}$-$^2P_{3/2}$, (e) $^2D_{5/2}$-$^2P_{3/2}$, (f) $^4S_{3/2}$-$^2P_{1/2}$, (g) $^4S_{3/2}$-$^2D_{5/2}$, (h) $^2D_{3/2}$-$^2P_{1/2}$, and (i) $^4S_{3/2}$-$^2P_{3/2}$.

This work was supported by the U.S. Department of Energy, Fundamental Interactions Branch, Office of Basic Energy Sciences, Division of Chemical Sciences, under Grant No. DE-FG05-88ER13958. One of us (Z.B.R.) gratefully acknowledges the support and hospitality provided to him at the University of Toledo.

*Permanent address: Institute of Theoretical Physics and Astronomy of the Lithuanian Academy of Sciences, A. Gostauto 12, Vilnius 232600, Lithuania.

[1] B. Edlén, in Spektroskopie I, edited by S. Flügge, Handbuch der Physik Vol. 27 (Springer, Berlin, 1964), pp. 80–220.

[2] L. J. Curtis, Phys. Rev. A **40**, 6958 (1989); J. Phys. B **22**, L267 (1989); Phys. Scr. **43**, 137 (1991).

[3] R. D. Cowan, *The Theory of Atomic Structure and Spectra* (University of California Press, Berkeley, 1981).

[4] E. U. Condon and G. H. Shortley, *The Theory of Atomic Spectra* (Cambridge University Press, Cambridge, 1935).

[5] M. W. Keller, *College Algebra* (Houghton Mifflin, Boston, 1946), p. 324.

[6] See references given by C. E. Theodosiou, Phys. Rev. A **30**, 2881 (1984).

[7] S. Pasternack, Astrophys. J. **92**, 129 (1940); G. H. Shortley, Phys. Rev. **57**, 225 (1940).

[8] C. Corliss and J. Sugar, J. Phys. Chem. Ref. Data **11**, 226 (1982).

[9] K. T. Cheng, Y.-K. Kim, and J. P. Desclaux, Atom. Data Nucl. Data Tables **24**, 111 (1979).

[10] K.-N. Huang, Atom. Data Nucl. Data Tables **30**, 313 (1984).

[11] S. T. Maniak and L. J. Curtis, Phys. Rev. A **42**, 1821 (1990).